The 2010 IEEE/RSJ International Conference on
Intelligent Robots and Systems
October 18-22, 2010, Taipei, Taiwan

Derivation of Optimal Robust Grasping Strategy under Initial Object Pose Errors

Hiroki Dobashi, Akio Noda, Yasuyoshi Yokokohji,
Hikaru Nagano, Tatsuya Nagatani, and Haruhisa Okuda

Abstract— **In a robotic cell, an assembly robot has to grasp various parts robustly even under some uncertainties in their initial poses. For this purpose, it is necessary to design robust grasping strategies for robotic hands. In this paper, we propose a method to derive an optimal robust grasping strategy from a given initial pose error region of a target object. Based on the pushing operation analysis, it is possible to simulate multi-fingered hand grasping and derive a permissible initial pose error region of a target object from which planned grasping is successful. Adopting an active search algorithm proposed by the authors, we can find the optimal grasping strategy efficiently. As an example, we derive the optimal grasping strategy for grasping a circular object by a three-fingered hand.**

I. INTRODUCTION

Recently in the manufacturing domain, cell production systems, where just a small group of workers (or even one worker) assemble a product from start to finish, have been adopted for products in wide variations but in small quantities and a short product cycle. Some cell production systems are automated by using robots, i.e., robotic cells. These robots currently use a number of grippers customized for various part shapes, but due to the cost and lack of versatility, it is required to introduce universal robotic hands. In addition, the assembly robot has to grasp various parts with planned poses (positions and orientations) relative to the hands even under some uncertainties in their initial poses. For example, uncertainties arise as errors due to rough supply by part feeders. To compensate for such uncertainties, visual sensors could be employed. However, the tact time may increase because of the required time for image recognition, and it is difficult to achieve the recognition accuracy needed for parts mating by visual sensors alone. From those reasons, it is also necessary to design robust grasping strategies for universal robotic hands by which planned grasping configuration is ensured without the aid of visual sensors even when parts have some initial pose errors.

This work is supported in part by New Energy and Industrial Technology Development Organization (NEDO) in Japan, under the Development Project of Intelligent Technology for Next-generation Robots.

H. Dobashi is with the Dept. of Mechanical Engineering and Science, Graduate School of Engineering, Kyoto University, Kyoto, 606-8501, Japan hiroki.dobashi@t03.mbox.media.kyoto-u.ac.jp

A. Noda, H. Nagano, T. Nagatani, and H. Okuda are with Advanced Technology R&D Center, Mitsubishi Electric Corporation, Hyogo, 661-8661, Japan {noda.akio@dh, Nagano.Hikaru@ze, Nagatani.Tatsuya@aj, Okuda.Haruhisa@ct}.MitsubishiElectric.co.jp

Y. Yokokohji is with the Dept. of Mechanical Engineering, Graduate School of Engineering, Kobe University, Hyogo, 657-8501 Japan yokokohji@mech.kobe-u.ac.jp

In our previous work [1], we proposed a systematic design methodology of universal hands for robotic cells. We assumed form closure grasp [2][3] because frictionless contacts between fingers and parts are beneficial for absorbing the initial pose errors of the parts during grasping. The proposed methodology, however, focused only on the final grasping configuration and did not consider the grasping strategy, i.e., how each finger should be moved toward the final grasping configuration to absorb the initial pose errors.

When a hand grasps a target object on a flat floor such as a workbench, pushing operations are the most primitive phenomena. Based on the pushing operation analysis, it is possible to calculate the object motion under a given grasping strategy and derive an initial pose error region of the object from which planned grasping is successful (we call it a "forward problem"). To design a robust grasping strategy under the initial object pose errors, it is necessary to derive a grasping strategy that can absorb a given initial pose error region (we call it an "inverse problem"). However, inverse problems cannot be solved directly due to the complex relation between a grasping strategy and an initial pose error region. Thus, it should be solved indirectly by searching solutions of the forward problems.

This paper proposes a method to derive a robust grasping strategy. First, pushing operations by multiple fingers under the quasi-static condition are analyzed. Then, based on the analysis, grasping simulations under given grasping strategies are conducted, and permissible initial pose error regions of a target object are derived from the simulation results. In addition, a numerically obtained permissible initial pose error region is verified experimentally. Finally, the method to derive an optimal robust grasping strategy under a given initial pose error region is proposed, and it is shown that the optimization is achieved efficiently with an active search algorithm proposed by the authors.

II. RELATED WORKS

Pushing operations have been analyzed by several researchers. MacMillan analyzed the motion of an object sliding on a frictional flat floor, and introduced the center of friction (COF) [4]. Mason discussed the basic mechanics of pushing operations [5]. Yoshikawa *et al.* proposed a method to identify the COF of an object by pushing it with an unknown friction distribution [6]. Bernheisel *et al.* [7] and Harada *et al.* [8] analyzed pushing operations of multiple objects. Object motions are usually assumed to be quasi-static [4]-[8], but Jia *et al.* analyzed the dynamics of pushing

operations [9].

Peshkin *et al.* discussed methods to align an object by finding the locus of the centers of rotation (CORs) of the object for all possible pressure distributions [10]. Kurisu *et al.* [11] and Akella *et al.* [12] proposed trajectory planning methods to move an object toward a final configuration by pushing operations. Brost [13] and Goldberg [14] discussed algorithms to orient any two-dimensional (2-D) polygonal part with an unknown initial pose toward its goal pose by a simple parallel-jaw gripper. Balorda *et al.* [15] proposed a method to eliminate uncertainties of the initial pose of an polygonal object by pushing with two point contacts. Maeda *et al.* analyzed graspless manipulation including pushing operations, and proposed manipulation planning to move an object robustly against disturbance [16]. Quasi-static motions are also supposed in [10]-[16].

For dealing with our problem, it is necessary to analyze pushing operations with multiple frictionless contacts between the object and the fingers. However, pushing operations with just a single [4]-[6][9]-[11] or two point contacts [15] have been discussed so far. Multiple contacts are assumed in [7][8][12]-[14][16], but they only discuss the cases using simple flat fences or parallel-jaw grippers, or the cases assuming frictional contacts between the object and the fingers. Thus, these are not applicable to our problem.

To achieve planned grasping accurately, influences of dynamical factors such as inertia and collisions between the object and the fingers should be minimized. In addition, quasi-static analysis is much simpler than dynamic one discussed in [9]. Therefore, quasi-static analysis is conducted in this paper like the most of other literature.

III. PUSHING OPERATION ANALYSIS AND GRASPING SIMULATION

In this section, pushing operations are analyzed, and then grasping simulations based on the analysis are conducted.

Actual parts may have various shapes, but some of them can be assumed to be prismatic. Grasping operations of those prismatic parts can be treated as 2-D problems [1]. Similarly, pushing operations are discussed as 2-D problems.

A. Conditions

The horizontal plane supporting a pushed object is called a supporting surface, and the following conditions are assumed:

1. The object is a 2-D rigid body with a known shape;
2. The coefficient of friction and the pressure distribution between the object and the supporting surface are known and constant;
3. Frictional forces between the object and the supporting surface are governed by the Coulomb's law;
4. Object motions are quasi-static and inertial forces and moments applied to the object are negligible compared to frictional forces (quasi-static condition);
5. The hand has multiple fingers and only the motions of their fingertips, which are also 2-D rigid bodies, are considered in the simulation;
6. The fingers make frictionless contacts with the object at finite points.

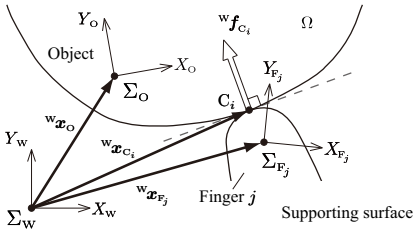

Fig. 1. Definition of coordinate systems and parameters

B. Formulation of Pushing Operation Problem

In this section, formulation to calculate the pushed object motion under given multiple-finger motions (pushing operation problem) is given.

Let n_{c} be the total number of contact points at which contact forces are applied to the object by the fingers, and C_i be the i-th contact point ($i = 1, 2, ..., n_{\mathrm{c}}$). Similarly, let n_{F} be the total number of fingers. If the j-th finger ($j = 1, 2, ..., n_{\mathrm{F}}$) has the i-th contact point C_i, let $k(i)$ denote the sequence number of this finger, i.e., $k(i) = j$. Besides, as shown in Fig. 1, a world coordinate frame Σ_{W}, an object coordinate frame Σ_{O}, and a finger coordinate frame Σ_{F_j} are attached to the supporting surface, the object, and finger j ($j = 1, 2, ..., n_{\mathrm{F}}$), respectively.

Let ${}^{\mathrm{W}}\boldsymbol{v}_{\mathrm{O}}$ be the velocity of the object at the origin of Σ_{O} with respect to Σ_{W}, and ω_{O} be its angular velocity (scalar value) relative to the supporting surface. When the fingers keep all of the n_{c} contacts with the object, the normal component of the finger velocity at C_i ($i = 1, 2, ..., n_{\mathrm{c}}$) on the finger contour equals to that of the object. Thus, we get

$$\boldsymbol{A} \begin{bmatrix} {}^{\mathrm{W}}\boldsymbol{v}_{\mathrm{O}} \\ \omega_{\mathrm{O}} \end{bmatrix} = \boldsymbol{b}, \tag{1}$$

where $\boldsymbol{A}$ and $\boldsymbol{b}$ are given by the following equations:

$$\boldsymbol{A} = [\, \boldsymbol{a}_1,\, \boldsymbol{a}_2,\, ...,\, \boldsymbol{a}_{n_{\mathrm{c}}} \,]^T,$$

$$\boldsymbol{b} = [\, b_1,\, b_2,\, ...,\, b_{n_{\mathrm{c}}} \,]^T,$$

$$\boldsymbol{a}_i = \begin{bmatrix} {}^{\mathrm{W}}\boldsymbol{n}_{\mathrm{C}_i} \\ ({}^{\mathrm{W}}\boldsymbol{x}_{\mathrm{C}_i} - {}^{\mathrm{W}}\boldsymbol{x}_{\mathrm{O}}) \times {}^{\mathrm{W}}\boldsymbol{n}_{\mathrm{C}_i} \end{bmatrix},$$

$$b_i = \begin{bmatrix} {}^{\mathrm{W}}\boldsymbol{n}_{\mathrm{C}_i} \\ ({}^{\mathrm{W}}\boldsymbol{x}_{\mathrm{C}_i} - {}^{\mathrm{W}}\boldsymbol{x}_{\mathrm{F}_{k(i)}}) \times {}^{\mathrm{W}}\boldsymbol{n}_{\mathrm{C}_i} \end{bmatrix}^T \begin{bmatrix} {}^{\mathrm{W}}\boldsymbol{v}_{\mathrm{F}_{k(i)}} \\ \omega_{\mathrm{F}_{k(i)}} \end{bmatrix}$$

$$(i = 1, 2, ..., n_{\mathrm{c}}). \tag{2}$$

In the above equations, ${}^{\mathrm{W}}\boldsymbol{n}_{\mathrm{C}_i}$ is the outward normal vector of the finger contour at contact point C_i. Vectors ${}^{\mathrm{W}}\boldsymbol{x}_{\mathrm{C}_i}$, ${}^{\mathrm{W}}\boldsymbol{x}_{\mathrm{O}}$, and ${}^{\mathrm{W}}\boldsymbol{x}_{\mathrm{F}_{k(i)}}$ denote the positions of contact point C_i, the origin of Σ_{O}, and the origin of $\Sigma_{\mathrm{F}_{k(i)}}$ with respect to Σ_{W}. Vector ${}^{\mathrm{W}}\boldsymbol{v}_{\mathrm{F}_{k(i)}}$ and scalar value $\omega_{\mathrm{F}_{k(i)}}$ are the velocity of finger $k(i)$ at the origin of $\Sigma_{\mathrm{F}_{k(i)}}$ with respect to Σ_{W} and its angular velocity relative to the supporting surface, respectively. Note that '$\times$' gives a scalar cross product of a pair of 2-D vectors $\boldsymbol{\alpha} = [\, \alpha_x,\, \alpha_y \,]^T$ and $\boldsymbol{\beta} = [\, \beta_x,\, \beta_y \,]^T$ by $\boldsymbol{\alpha} \times \boldsymbol{\beta} = \alpha_x \beta_y - \alpha_y \beta_x$.

Next, the equilibrium of the forces and moments applied to the object is described.

Let ${}^{\mathrm{W}}\boldsymbol{f}_{\mathrm{C}_i}$ be the contact force applied to the object by the finger $k(i)$ at contact point C_i with respect to Σ_{W}, and $m_{\mathrm{C}_i,\mathrm{O}}$ be the moment (scalar value) applied to the object around the vertical axis passing through the origin of Σ_{O} by ${}^{\mathrm{W}}\boldsymbol{f}_{\mathrm{C}_i}$ ($i = 1, 2, ..., n_{\mathrm{c}}$). Similarly, let ${}^{\mathrm{W}}\boldsymbol{f}_{\mathrm{S}}$ be the total frictional force applied to the object by the supporting surface with respect to Σ_{W}, and $m_{\mathrm{S,O}}$ be the total frictional moment (scalar value) applied to the object from the supporting surface around the vertical axis passing through the origin of Σ_{O}.

From Condition 4 in Section III-A, we have the following equilibrium equation of the forces and moments applied to the object:

$$\sum_{i=1}^{n_{\mathrm{c}}} \begin{bmatrix} {}^{\mathrm{W}}\boldsymbol{f}_{\mathrm{C}_i} \\ m_{\mathrm{C}_i,\mathrm{O}} \end{bmatrix} + \begin{bmatrix} {}^{\mathrm{W}}\boldsymbol{f}_{\mathrm{S}} \\ m_{\mathrm{S,O}} \end{bmatrix} = \boldsymbol{0}. \tag{3}$$

From Condition 6 in Section III-A, we get

$${}^{\mathrm{W}}\boldsymbol{f}_{\mathrm{C}_i} = f_{\mathrm{C}_i}\, {}^{\mathrm{W}}\boldsymbol{n}_{\mathrm{C}_i}, \tag{4}$$

where f_{C_i} ($f_{\mathrm{C}_i} > 0$) is the magnitude of contact force ${}^{\mathrm{W}}\boldsymbol{f}_{\mathrm{C}_i}$. The total frictional force ${}^{\mathrm{W}}\boldsymbol{f}_{\mathrm{S}}$ is given by

$${}^{\mathrm{W}}\boldsymbol{f}_{\mathrm{S}} = -\int_{\Omega} \mu_{\mathrm{P}} p_{\mathrm{P}}\, {}^{\mathrm{W}}\hat{\boldsymbol{v}}_{\mathrm{P}}\, d\Omega. \tag{5}$$

The domain of integration Ω is the contact region between the object and the supporting surface. In (5), μ_{P} and p_{P} are the coefficient of friction between the object and the supporting surface, and the normal force density (pressure) applied to the object from the supporting surface at a point P in Ω. In addition, ${}^{\mathrm{W}}\hat{\boldsymbol{v}}_{\mathrm{P}}$ is a unit vector parallel to the object velocity at a point P in Ω with respect to Σ_{W}, and it is given by

$${}^{\mathrm{W}}\hat{\boldsymbol{v}}_{\mathrm{P}} = \frac{{}^{\mathrm{W}}\boldsymbol{v}_{\mathrm{O}} + \omega_{\mathrm{O}} \otimes ({}^{\mathrm{W}}\boldsymbol{x}_{\mathrm{P}} - {}^{\mathrm{W}}\boldsymbol{x}_{\mathrm{O}})}{|| {}^{\mathrm{W}}\boldsymbol{v}_{\mathrm{O}} + \omega_{\mathrm{O}} \otimes ({}^{\mathrm{W}}\boldsymbol{x}_{\mathrm{P}} - {}^{\mathrm{W}}\boldsymbol{x}_{\mathrm{O}}) ||}, \tag{6}$$

where ${}^{\mathrm{W}}\boldsymbol{x}_{\mathrm{P}}$ represents the position of a point P in Ω with respect to Σ_{W}. Note that '$\otimes$' denotes a 2-D vector cross product operation defined as $\alpha \otimes \boldsymbol{\beta} = \alpha\,[-\beta_y,\ \beta_x]^T$ with a scalar α and a 2-D vector $\boldsymbol{\beta} = [\beta_x,\ \beta_y]^T$. The moment $m_{\mathrm{C}_i,\mathrm{O}}$ and the total frictional moment $m_{\mathrm{S,O}}$ are given by

$$m_{\mathrm{C}_i,\mathrm{O}} = ({}^{\mathrm{W}}\boldsymbol{x}_{\mathrm{C}_i} - {}^{\mathrm{W}}\boldsymbol{x}_{\mathrm{O}}) \times {}^{\mathrm{W}}\boldsymbol{f}_{\mathrm{C}_i}, \tag{7}$$

$$m_{\mathrm{S,O}} = -\int_{\Omega} \mu_{\mathrm{P}} p_{\mathrm{P}}\, ({}^{\mathrm{W}}\boldsymbol{x}_{\mathrm{P}} - {}^{\mathrm{W}}\boldsymbol{x}_{\mathrm{O}}) \times {}^{\mathrm{W}}\hat{\boldsymbol{v}}_{\mathrm{P}}\, d\Omega. \tag{8}$$

Substituting (4) into (3) and rearranging the terms, we get

$$\boldsymbol{A}^T \boldsymbol{f} = \boldsymbol{d}, \tag{9}$$

where $\boldsymbol{f} = [\, f_{\mathrm{C}_1},\ f_{\mathrm{C}_2},\ ...,\ f_{\mathrm{C}_{n_{\mathrm{c}}}}\,]^T$ and $\boldsymbol{d} = -[\, {}^{\mathrm{W}}\boldsymbol{f}_{\mathrm{S}}^T,\ m_{\mathrm{S,O}}\,]^T$.

By solving (1) and (9) for ${}^{\mathrm{W}}\boldsymbol{v}_{\mathrm{O}}$ and ω_{O}, the solution of a pushing operation problem, i.e., the motion of a target object can be obtained. Since the details of how to solve the equations are not the main topics of this paper, they are not shown here (see [17] for more details).

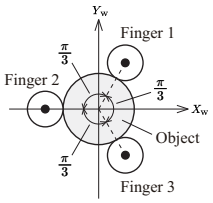

Fig. 2. Final grasping configuration of a circular object

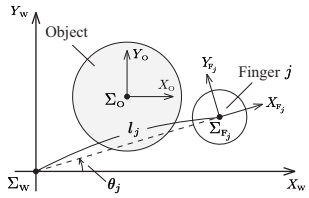

Fig. 3. Coordinate frames of a circular object and finger j

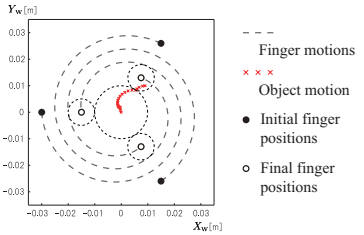

Fig. 4. Result of a circular object grasping simulation

C. Grasping Simulation

Based on the formulation discussed in the previous section, it is possible to simulate the motion of an object in the process of grasping by a multi-fingered hand. In this section, grasping simulations of circular and polygonal objects are shown as examples.

To simplify the problems, all of the fingers of a hand are assumed to be circular (radius r_{F}). Practically speaking, circular fingers would be beneficial in a sense of versatility because it is not necessary to care their orientations. In addition, it is assumed that both the coefficient of friction μ_{P} and the pressure distribution p_{P} are uniform over the contact region Ω.

First, grasping of a circular object (radius r_{O}) is discussed. Since frictionless contacts between the fingers and the object are assumed as stated in Condition 6 in Section III-A, contact points must be chosen so that they achieve a form-closure grasp. In the case of a circular object, however, we cannot find such contact points (there is no constraint on the object rotation) [3]. Then, we assume three contact points that achieve a form-closure grasp only in the translational components as shown in Fig. 2.

As shown in Fig. 3, the object frame Σ_{O} is attached to the center of the object, and finger frame Σ_{F_j} ($j = 1, 2, 3$) is attached to the center of finger j. For the later discussion in Section IV-A, it is assumed that finger j moves in such a way that the negative direction of axis X_{F_j} always points the origin of the world frame Σ_{W}. Let l_j be the length of the line segment between the origins of Σ_{W} and Σ_{F_j}, and θ_j be the angle of this line segment from axis X_{W}.

According to the definition of the COF [6], the COF of a circular object with uniform coefficient of friction and pressure distribution is located at the center of the object. Since the fingers make frictionless contacts with the object, all the lines of action of ${}^{\mathrm{W}}\boldsymbol{f}_{\mathrm{C}_i}$ ($i = 1, 2, ..., n_{\mathrm{c}}$) always pass through the COF. In this case, the object only translates [18].

A simulation result is shown in Fig. 4. The values of the parameters are $r_{\mathrm{O}} = 0.01$ [m], $r_{\mathrm{F}} = 0.005$ [m], $\dot{l}_j = -1.875 \times$

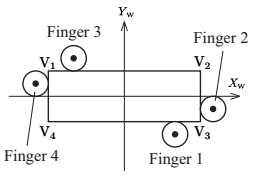

Fig. 5. Final grasping configuration of a rectangular object

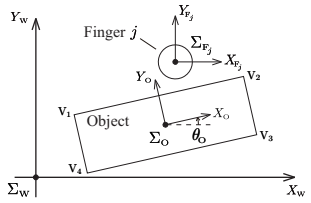

Fig. 6. Coordinate frames of a rectangular object and finger $\boldsymbol{j}$

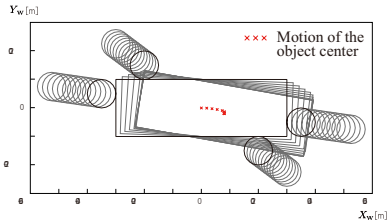

Fig. 7. Result of a rectangular object grasping simulation

$10^{-3}\,[\mathrm{m/s}]$, $\dot{\theta}_j = \pi/4\,[\mathrm{rad/s}]$ ($j = 1, 2, 3$), and the initial conditions are ${}^{\mathrm{W}}\boldsymbol{x}_{\mathrm{O}} = [\,0.009,\ 0.01\,]^T\,[\mathrm{m}]$, $l_j = 0.03\,[\mathrm{m}]$, $\theta_j = (2j-1)\pi/3\,[\mathrm{rad}]$ ($j = 1, 2, 3$). When using MATLAB on a PC with Core 2 Duo P9500 2.53 [GHz] and setting the time step as $1.0 \times 10^{-3}\,[\mathrm{s}]$, the simulation time was $0.776\,[\mathrm{s}]$.

Second, polygonal object grasping is discussed. As a simple example, grasping of a rectangular object by form closure as shown in Fig. 5 is considered.

As shown in Fig. 6, the object frame Σ_{O} is attached to the geometric center of the object in such a way that the positive direction of axis X_{O} is parallel to the direction from vertex V_1 to V_2, and let θ_{O} be the angle of axis X_{O} from axis X_{W}. Again, according to the definition of the COF [6], the COF of a rectangular object with uniform coefficient of friction and pressure distribution is located at the geometric center of the object. However, when grasping a polygonal object including a rectangular object, the lines of action of ${}^{\mathrm{W}}\boldsymbol{f}_{\mathrm{C}_i}$ ($i = 1, 2, ..., n_{\mathrm{c}}$) do not always pass through the COF while they do in the case of circular object grasping. Thus, the object may have a rotational motion component [18]. Finger frame Σ_{F_j} ($j = 1, 2, 3, 4$) is attached to the center of finger j.

The sequence of rectangular object grasping is illustrated in Fig. 7. The values of the parameters are $r_{\mathrm{F}} = 0.005\,[\mathrm{m}]$, $\mathrm{V}_1\mathrm{V}_2 = \mathrm{V}_3\mathrm{V}_4 = 0.06\,[\mathrm{m}]$, $\mathrm{V}_2\mathrm{V}_3 = \mathrm{V}_1\mathrm{V}_4 = 0.02\,[\mathrm{m}]$, and the initial pose of of the object is ${}^{\mathrm{W}}\boldsymbol{x}_{\mathrm{O}} = [\,0.008,\ -0.002\,]^T\,[\mathrm{m}]$ and $\theta_{\mathrm{O}} = -\pi/18\,[\mathrm{rad}]$. The grasping strategy used in the simulation is described as ${}^{\mathrm{W}}\boldsymbol{v}_{\mathrm{F}_1} = -{}^{\mathrm{W}}\boldsymbol{v}_{\mathrm{F}_3} = [\,-0.004,\ 0.003\,]^T\,[\mathrm{m/s}]$, ${}^{\mathrm{W}}\boldsymbol{v}_{\mathrm{F}_2} = -{}^{\mathrm{W}}\boldsymbol{v}_{\mathrm{F}_4} = [\,-0.007,\ 0.001\,]^T\,[\mathrm{m/s}]$, under the initial condition where ${}^{\mathrm{W}}\boldsymbol{x}_{\mathrm{F}_1} = -{}^{\mathrm{W}}\boldsymbol{x}_{\mathrm{F}_3} = [\,0.03,\ -0.0225\,]^T\,[\mathrm{m}]$, ${}^{\mathrm{W}}\boldsymbol{x}_{\mathrm{F}_2} = -{}^{\mathrm{W}}\boldsymbol{x}_{\mathrm{F}_4} = [\,0.0525,\ -0.0075\,]^T\,[\mathrm{m}]$. When using MATLAB on the PC used in the circular object grasping simulation and setting the time step as $2.0 \times 10^{-3}\,[\mathrm{s}]$, the simulation time was $36.5\,[\mathrm{s}]$. The reason for the great difference of the simulation time from that of the previous simulation is the necessity to solve the nonlinear equation (9). See [17] for more details.

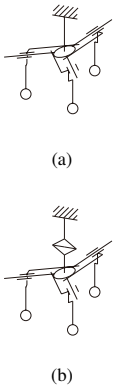

Fig. 8. Three-fingered chuck-type hands for grasping a circular object

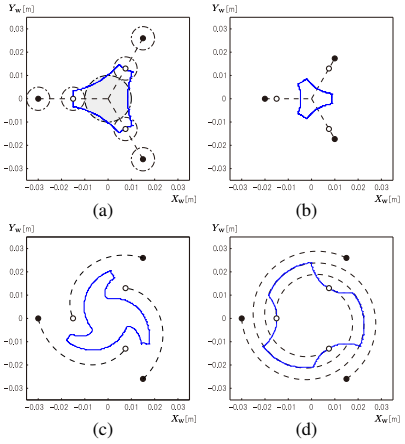

Fig. 9. Permissible initial pose (position) error regions of a circular object

TABLE I

VALUES OF THE PARAMETERS

Parameter ($j = 1, 2, 3$)	(a)	(b)	(c)	(d)
$l_j\vert_{t=0}$ [m]	0.03	0.02	0.03	0.03
$-\dot{l}_j \times 10^{-3}$ [m/s]	1.875	1.875	5.625	1.875
$\dot{\theta}_j$ [rad/s]	0	0	$\pi/4$	$\pi/4$

IV. PERMISSIBLE INITIAL POSE ERROR REGION

Repeating the grasping simulation from a different initial pose from the previous ones, it is possible to find a permissible initial pose error region of a target object from which planned grasping is successful. In the following sections, such regions of circular and rectangular objects are discussed as examples. Then, a numerically obtained region of a circular object is verified experimentally.

A. Simulation

In this section, permissible initial pose error regions of circular and rectangular objects are found by the grasping simulation. Note that the definition of the parameters used in this section follows that in Section III-C.

First, that of a circular object is discussed. According to the design framework proposed in [1], a three-fingered chuck-type hand as shown in Fig. 8 (a) is considered as a minimally necessary mechanism for grasping a circular object. Permissible initial pose error regions of a circular object grasped by a chuck-type hand with different grasping strategies are shown in Figs. 9 (a) through (d). In the case of (c) and (d), an additional degree of freedom (DOF) of rotation around the normal axis of the supporting surface is assumed as shown in Fig. 8 (b). Note that most of industrial robots can make such a motion by their last joint. Table I shows the values of the parameters used in the simulations. In the table, $l_j\vert_{t=0}$ denotes the value of l_j at the initial time $t = 0$. Note that these values describe grasping strategies. The radii of the circular object and the fingers are the same as in Section III-C.

In Fig. 9, the permissible initial pose error region is given as an area surrounded by a solid line. Small solid circles denote the initial positions of the fingers and open circles are

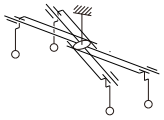

Fig. 10. Chuck-type hand for grasping a rectangular object

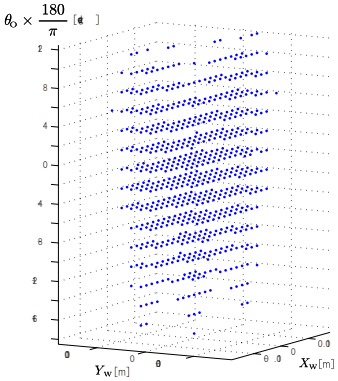

Fig. 11. Permissible initial pose error region of a rectangular object

their final positions. Dashed lines from the initial positions to the final ones show the finger trajectories. The fingertip contours (dashed-dotted circles) and the object contour (a dashed-dotted circle filled with gray color) are drawn only in Fig. 9 (a). Note that orientational errors are not considered here because the orientation of a circular object can never be kinematically constrained.

Comparing Fig. 9 (a) with (b), it can be seen that the permissible initial pose error region can be enlarged by making the finger stroke longer. When the additional rotational joint is introduced, the region is drastically enlarged as seen in Fig. 9 (d). However, the pitch of the spiral trajectory must be small enough to get a large region. This can be achieved by setting the ratio of $|\dot{\theta}_j|$ to $|\dot{l}_j|$ large. When the pitch is not so small, the resultant region becomes small as seen in Fig. 9 (c) and cannot cover the region shown in Fig. 9 (a).

Similarly to the case of circular object grasping, the permissible initial pose error region of a rectangular object can be obtained. Again, according to the design framework proposed in [1], a four-fingered chuck-type hand as shown in Fig. 10 is considered as a minimally necessary mechanism for grasping a rectangular object.

Figure 11 illustrates the obtained permissible initial pose error region of a rectangular object by a set of grid points each of which is represented by a small solid circle. In the case of a rectangular object, not only translational errors but also rotational ones must be considered, unlike the case of the circular object. Thus, the permissible initial pose error region is represented in three dimensions. The grasping strategy used in the simulation is given in the same way as in the grasping simulation shown in Section III-C.

B. Experimental Verification

In this section, a numerically obtained permissible initial pose error region is verified experimentally. As an example, a grasping experiment of a cylindrical object with a chuck-type hand as shown in Fig. 8 (a) is conducted, and the permissible initial pose error region shown in Fig. 9 (a) is verified. Note that grasping a cylindrical object corresponds to grasping a circular object in two dimensions.

The experimental setup is shown in Fig. 12. A cylindrical object $0.02\,[\mathrm{m}]$ in diameter made of polyoxymethylene

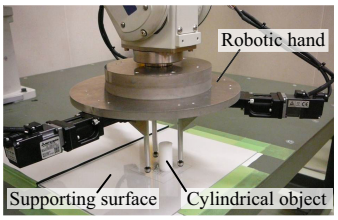

Fig. 12. Experimental setup

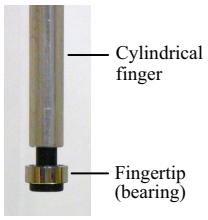

Fig. 13. Finger part

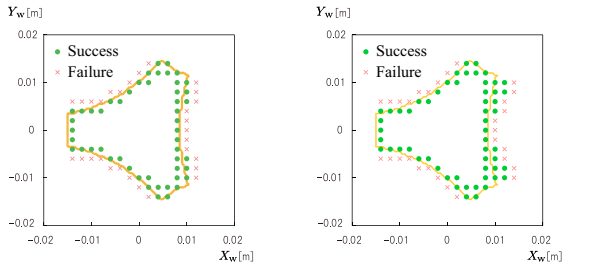

(a) Frictionless fingertip (with bearing) (b) Normal fingertip (without bearing)

Fig. 14. Experimental results

(POM) is used as a target object. The height of the object is $0.042\,[\mathrm{m}]$, and its mass is $19.5 \times 10^{-3}\,[\mathrm{kg}]$. The supporting surface is made of acrylate resin (Mitsubishi Rayon).

The experimental chuck-type hand is attached to a six-axis manipulator (MITSUBISHI, MELFA RV-6SL). It has three pairs of a ball screw unit (MISUMI, LX2001-B1-A2028-100) and a servo motor (MITSUBISHI, HC-AQ0135D) which are synchronized so that the DOF of the hand is regarded as one.

A cylindrical finger and fingertip as shown in Fig. 13 are mounted in each ball screw unit. In this research, frictionless contacts between the fingers and the object are assumed as stated in Condition 6 in Section III-A. However, it is an ideal condition, and some friction exists in reality. To eliminate the influence of the friction, a stainless-steel bearing (MISUMI, SBR105ZZ) is used as each fingertip as shown in Fig. 13. The bearing is $0.01\,[\mathrm{m}]$ in diameter and $0.004\,[\mathrm{m}]$ in thickness. The influence of the friction between the fingers and the object parallel to the supporting surface is eliminated, but the bearings can still apply some frictional forces to the object in the vertical direction and thus the hand can pick up the object. For comparison, the normal fingertips without bearings with the same dimension are also used as frictionless fingertips.

In the experiment, it is checked if the cylindrical object located at a point on the supporting surface can be grasped. Every grid points with $0.002\,[\mathrm{m}]$ intervals near the boundary of the region shown in Fig. 9 (a) is tested once. The finger speed is set as $1.875 \times 10^{-3}\,[\mathrm{m/s}]$, and each finger is made to contact the object near its bottom (about $0.008\,[\mathrm{m}]$ above the supporting surface) to maintain a stable pushing motion.

The experimental results with the frictionless fingertips and the normal ones are shown in Figs.14 (a) and (b). In the figures, each small solid circle shows the initial position from which the grasping is successful, and each 'x' shows the one in failure. Note that initial positions where the fingers interfere with the object are not plotted. For comparison, the boundary of the initial pose error region shown in Fig. 9

(a), which is derived using grid points with 5.0×10^{-4} [m] intervals, is also plotted.

As can be seen in Fig. 14, both the experimentally obtained permissible initial pose error regions with the frictionless fingertips and the normal fingertips are almost identical to the numerical one. It means that the correctness of the numerical region is confirmed. The reason why the region in Fig. 14 (b) differs from the numerical one more than that in Fig. 14 (a) is considered as the influence of the friction between the fingertips and the object.

V. OPTIMIZATION OF GRASPING STRATEGY

In this section, a method to derive an optimal robust grasping strategy under a given initial pose error region is proposed. As an example, circular object grasping is discussed, and it is shown that the optimization is achieved efficiently with an active search algorithm.

A. Definition of Optimal Robust Grasping Strategy

To achieve planned grasping robustly, it is necessary to absorb initial pose errors of a target object. In addition, it is desirable to minimize the required time for robust grasping. There is a trade-off relation between these two conditions. For example, in Fig. 9, the permissible initial pose error region in (d) is larger than that in (c) while the required time for grasping of (c) is shorter than (d).

From this point of view, the optimal grasping strategy is defined as one that can meet both of these two conditions.

B. Active Search Algorithm

As mentioned in Section I, an optimal grasping strategy is expected to be found by searching solutions of the forward problems. In order to lower the searching cost, an active search algorithm proposed by Noda *et al* [19] is adopted. The main idea of the algorithm is to find an optimal set of control parameters efficiently by using an optimal sample set of the control parameters in each sequential trial. The details of the algorithm are discussed below.

Letting $\boldsymbol{x}$ be control parameters of a target system, the algorithm is used to find the optimal values of the parameters $\boldsymbol{x}$ so that they maximize the value of an objective function $F(\boldsymbol{x})$ under a constraint $f(\boldsymbol{x}) > 0$ by sequential trials. The algorithm is effective for the case where the objective function $F(\boldsymbol{x})$ has the maximum value near the boundary of the constraint, i.e., $f(\boldsymbol{x}) = 0$ even when the function forms of $F(\boldsymbol{x})$ and $f(\boldsymbol{x})$ are unknown.

In the algorithm, each sequential trial is conducted with the optimal sample of the parameters $\boldsymbol{x}$ chosen in the following procedure. When the n-th trial is conducted, estimation models, $F_n(\boldsymbol{x})$ and $f_n(\boldsymbol{x}) = 0$, which correspond to $F(\boldsymbol{x})$ and $f(\boldsymbol{x}) = 0$, are constructed. Then, using each of several candidates $\boldsymbol{s}_{n+1}$ for the sample used for the $(n+1)$-th trial, estimation model of $f(\boldsymbol{x}) = 0$ is constructed under each of the assumptions, $f_n(\boldsymbol{s}_{n+1}) > 0$ and $f_n(\boldsymbol{s}_{n+1}) < 0$. Let $g_{n+1}(\boldsymbol{s}_{n+1}, \boldsymbol{x}) = 0$ and $h_{n+1}(\boldsymbol{s}_{n+1}, \boldsymbol{x}) = 0$ be the estimation models for the respective assumptions. To estimate the boundary $f(\boldsymbol{x}) = 0$ of the constraint accurately, information

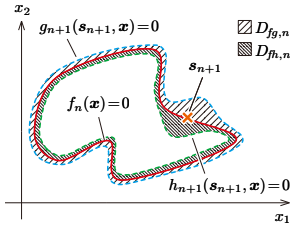

Fig. 15. Evaluation of the next sampling

obtained from the $(n+1)$-th trial with a sample $\boldsymbol{s}_{n+1}$ should be maximized. That is, both the difference between $f_n(\boldsymbol{x}) = 0$ and $g_{n+1}(\boldsymbol{s}_{n+1}, \boldsymbol{x}) = 0$, and that between $f_n(\boldsymbol{x}) = 0$ and $h_{n+1}(\boldsymbol{s}_{n+1}, \boldsymbol{x}) = 0$ should be as large as possible. Let $D_{fg,n}$ and $D_{fh,n}$ denote the quantities of the respective differences. For instance, the volume between the boundaries can be used for $D_{fg,n}$ and $D_{fh,n}$. In the 2-D case, where $\boldsymbol{x} = [\, x_1,\, x_2 \,]$, $D_{fg,n}$ and $D_{fh,n}$ represent the area between the respective boundaries as shown in Fig. 15. Besides, to maximize the value of the objective function $F(\boldsymbol{x})$, its value for $\boldsymbol{x} = \boldsymbol{s}_{n+1}$ needs to be as large as possible. Therefore, the optimal sample $\boldsymbol{s}^*_{n+1}$ defined by (10) is chosen and used for the $(n+1)$-th trial.

$$\boldsymbol{s}^*_{n+1} = \arg \max_{\boldsymbol{s}_{n+1}} \left\{ \frac{D_{fg,n} + D_{fh,n}}{|D_{fg,n} - D_{fh,n}| + 1} F_n(\boldsymbol{s}_{n+1}) \right\} \tag{10}$$

The term between the braces in the right side of (10) represents an evaluation index to choose the optimal sample.

Let $R_{\rm a}$ be the initial pose error region of a target object to be absorbed, $R_{\rm g}$ be the permissible error region, and T be the required time for grasping. According to the previous section, the constraint $f(\boldsymbol{x}) > 0$ corresponds to $R_{\rm a} \subseteq R_{\rm g}$, and the objective function $F(\boldsymbol{x})$ is set as $1/T$.

C. Example of Optimization

As an example, a robust grasping strategy for a circular object is considered. The definition of parameters and the goal grasp are set the same as in Sections III-C and IV-A. As control parameters, $\dot{l}_j$, $\dot{\theta}_j$, and $l_j|_{t=0}$ $(j = 1, 2, 3)$ are used. For simplification, the respective parameters are set the same for $j = 1, 2, 3$, and they are denoted by $\dot{l}$, $\dot{\theta}$, and l_0.

Figure 16 shows the result of an example simulation conducted using MATLAB on a PC with Dual-Core AMD Opteron 2220 2.8 [GHz]. The radii of the fingers and the object are $r_{\rm F} = 0.005$ [m] and $r_{\rm O} = 0.01$ [m]. The error region $R_{\rm a}$ is set as a circular region centered at the origin of the world frame $\Sigma_{\rm W}$ with radius 0.01 [m]. As for the control parameters, $\dot{l}$ with 0.0002 [m/s] increments between -0.003 [m/s] and -0.001 [m/s], $\dot{\theta}$ with $\pi/12$ [rad/s] increments between 0 [rad/s] and $\pi/2$ [rad/s], and l_0 with 0.002 [m] increments between 0.02 [m] and 0.04 [m] are used. That is, three-dimensional (3-D) search space with 847 $(= 11 \times 7 \times 11)$ combinations of the values of the parameters is used.

The solid line in Fig. 16 shows the transition of the value of the objective function, and the dashed line shows the simulation time. Note that the simulation is conducted for all the 847 combinations for reference, but practically the

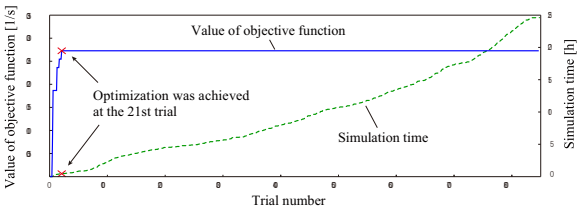

Fig. 16. Simulation result

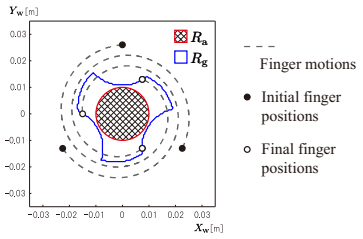

Fig. 17. Obtained optimum grasping strategy

simulation can be stopped when the value of the objective function hardly changes. As can be seen from Fig. 16, optimization is completed in the 21st trial. In the figure, '$\times$' shows each value of the objective function and the simulation time in the 21st trial. It can be seen that optimization of a robust grasping strategy is achieved efficiently by the active search algorithm. The values of the control parameters for the optimal grasping strategy are $\dot{l} = -0.003\,[\mathrm{m/s}]$, $\dot{\theta} = \pi/2\,[\mathrm{rad/s}]$, and $l_0 = 0.026\,[\mathrm{m}]$. The required time for the optimal grasping is $T = 3.67\,[\mathrm{s}]$. The finger trajectories and the regions R_a and R_g are shown in Fig. 17.

Only circular object grasping is discussed as an example here, but note that the proposed method can be applied to grasping of any shaped object. The only difference is that the initial pose error regions R_a and R_g are represented in three dimensions. Derivation of robust grasping strategies for various shaped objects is a future work.

VI. CONCLUSIONS AND FUTURE WORKS

In this paper, a method to derive a robust grasping strategy is proposed. First, acknowledging that pushing is the most primitive operation when a hand grasps a part on a flat floor, pushing operations by multiple fingers under the quasi-static condition are analyzed. Then, based on the analysis, grasping simulations of circular and rectangular objects under given grasping strategies are conducted, and permissible initial pose error regions are derived. One of the numerically obtained permissible initial pose error region of a circular object is verified experimentally with a cylindrical object, and it is shown that the experimentally obtained error region is almost identical to the numerical one. Finally, the method to derive an optimal robust grasping strategy under a given initial pose error region is proposed, and it is shown that the optimal strategy for circular object grasping can be obtained efficiently with the active search algorithm.

As future works, it is necessary to apply our proposed method to various shaped objects and verify the robustness of derived grasping strategies by real experiments, starting from grasping a primitive shape such as a cylinder and prisms, and hopefully trying some real product parts at the end. To make the pushing operation analysis more realistic, it would be necessary to consider frictional contacts between a target object and fingers, and nonuniform friction distribution between the object and the supporting surface. Then, a methodology to apply the robust grasping strategies obtained from our proposed method to designing universal robotic hands for a robotic cell should be discussed.

REFERENCES

[1] H. Dobashi, Y. Yokokohji, and K. Maekawa, "A Design Framework of Universal Hands for Robotic Cell Production Systems," *Proc. of the 25th Annual Conference of the Robotics Society of Japan*, 2007, 3M25 (in Japanese).

[2] F. Reuleaux, The Kinematics of Machinery, Macmillan, New York, 1876.

[3] X. Markenscoff, L. Ni, and C.H. Papadimitriou, "The geometry of grasping," *The International Journal of Robotics Research*, vol.9, no.1, 1990, pp.61-74.

[4] W.D. MacMillan, Dynamics of Rigid Bodies, Dover Publications, 1936.

[5] M.T. Mason, "Mechanics and Planning of Manipulator Pushing Operations," *The International Journal of Robotics Research*, vol.5, no.3, 1986, pp.53-71.

[6] T. Yoshikawa and M. Kurisu, "Identification of the Center of Friction from Pushing an Object by a Mobil e Robot," *Proc. of IEEE/RSJ International Workshop on Intelligent Robots and Syst ems*, 1991, pp.449-454.

[7] J.D. Bernheisel and K.M. Lynch, "Stable Transport of Assemblies: Pushing Stacked Parts," *IEEE Transactions on Automation Science and Engineering*, vol.1, no.2, 2004, pp.163-168.

[8] K. Harada, "Pushing Manipulation for Multiple Objects," *Transactions of the ASME*, vol.128, no.2, 2006, pp.422-427.

[9] Y.B. Jia and M. Erdmann, "Pose and Motion from Contact," *The International Journal of Robotics Research*, vol.18, no.5, 1999, pp.466-487.

[10] M.A. Peshkin, and A.C. Sanderson, "The Motion of a Pushed, Sliding Workpiece," *IEEE Journal of Robotics and Automation*, vol.4, no.6, 1988, pp.569-598.

[11] M. Kurisu and T. Yoshikawa, "Trajectory Planning for an Object in Pushing Operation," *Proc. of 1994 Japan-USA Symposium on Flexible Automation*, 1994, pp.1009-1016.

[12] S. Akella and M.T. Mason, "Posing Polygonal Objects in the Plane by Pushing," *The International Journal of Robotics Research*, vol.17, no.1, 1998, pp.70-88.

[13] R.C. Brost, "Automatic Grasp Planning in the Presence of Uncertainty," *The International Journal of Robotics Research*, vol.7, no.1, 1988, pp.3-17.

[14] K. Goldberg, "Orienting Polygonal Parts Without Sensors," *Algorithmica*, vol.10, 1993, pp.201-225.

[15] Z. Balorda and T. Bajd, "Reducing Positioning Uncertainty of Objects by Robot Pushing," *IEEE Transactions on Robotics and Automation*, vol.10, no.4, 1994, pp.535-541.

[16] Y. Maeda and T. Arai, "Planning of graspless manipulation by a multifingered robot hand," *Advanced Robotics*, vol.19, no.5, 2005, pp.501-521.

[17] H. Dobashi, Y. Yokokohji, A. Noda, and H. Okuda, "Permissible Initial Pose Error Region of an Object Grasped by a Universal Hand," *Proc. of 2010 International Symposium on Flexible Automation*, 2010, JPL-2452.

[18] H. Dobashi, Y. Yokokohji, A. Noda, and H. Okuda, "Multi-fingered Hand Grasping Simulation Based on Quasi-Static Pushing Operation Analysis and Derivation of Permissible Initial Error Regions of an Object," *Journal of the Robotics Society of Japan*, 2010 (to appear, in Japanese).

[19] A. Noda, T. Nagatani, H. Nagano, "Active Search Algorithm on Motion Learning of Industrial Robots," *Proc. of the 9th SICE System Integration Division Annual Conference*, 2008, 1E3-6, pp.211-212 (in Japanese).